Acta Cryst. (1993). D**49**, 541–547

Structure of the Crystalline Complex of Cytidylic Acid (2′-CMP) with Ribonuclease at 1.6 Å Resolution. Conservation of Solvent Sites in RNase-A High-Resolution Structures

BY J. N. LISGARTEN, V. GUPTA, D. MAES AND L. WYNS

Department of Ultrastructure, Instituut voor Molekulaire Biologie, Vrije Universiteit Brussel, B-1640 Sint Genesius Rode, Belgium

AND I. ZEGERS, R. A. PALMER,* C. G. DEALWIS, C. F. AGUILAR AND A. M. HEMMINGS

Department of Crystallography, Birkbeck College, University of London, London WC1E 7HX, England

(*Received* 22 *March* 1993; *accepted* 7 *July* 1993)

Abstract

The X-ray structure of the inhibitor complex of bovine ribonuclease A with cytidylic acid (2′-CMP) has been determined at 1.6 Å resolution and refined by restrained least squares to $R = 0.17$ for 11 945 reflections. Binding of the inhibitor molecule to the protein is confirmed to be in the productive mode associated with enzyme activity. A study of conserved solvent sites amongst high-resolution structures in the same crystal form reveals a stabilizing water cluster between the N and C termini.

Introduction

Bovine pancreatic ribonuclease A (RNase A; E.C. 3.1.4.22) is one of the most intensively studied enzymes (see for example the review of Blackburn & Moore, 1982). Its two-step catalytic cleavage of the phosphodiester bond of ribonucleotides is understood in some detail (Richards, Wyckoff, Allewell, Lee & Mitsui, 1971; Richards & Wyckoff, 1973; Wodak, Liu & Wyckoff, 1977; Pavlovsky, Borisova, Borisov, Antonov & Karpeisky, 1978) as depicted in Fig. 1. Recently a novel form of nucleotide binding to RNase has been observed in high-resolution studies of complexes formed with the inhibitors cytidylyl-2′,5′-guanosine (2′,5′-CpG) and deoxycytidylyl-3′,5′-guanosine (3′,5′-dCpdG), respectively. This non-productive binding mode has been dubbed retro-binding (Aguilar, Thomas, Moss, Mills & Palmer, 1992). These observations prompted a re-investigation of some mononucleotide–RNase complexes originally studied at low or intermediate resolution (Borkakoti, Palmer, Haneef & Moss, 1983; Howlin, Harris, Moss & Palmer, 1987; Palmer, Moss, Haneef & Borkakoti, 1984).

Here we report the X-ray analysis of cytidine-2′-phosphate (cytidylic acid or 2′-CMP), complexed with ribonuclease A. In order to obtain a reliable and detailed analysis it was decided to carry out this study at a resolution approaching the high-resolution native-protein study undertaken at 1.45 Å (Borkakoti, Moss & Palmer, 1982), using the protocol established successfully by Aguilar *et al.* (1992) for characterization of RNase–dinucleotide complexes. The present study is essentially an extension of the 2.3 Å resolution analysis of Howlin *et al.* (1987). It was undertaken to obtain confirmation of the productive mode of nucleotide binding in this complex; to gain, from the benefit of higher resolution data, a clearer picture of the ribose moiety (poorly resolved in the 2.3 Å study); to determine accurate geomet-

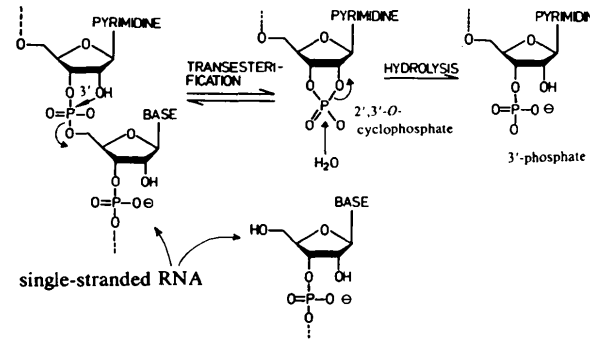

Fig. 1. Mechanism of pancreatic ribonuclease (RNase A): RNase A cleaves single-stranded RNA at the 3′-end of pyrimidine nucleosides. An RNA fragment with intermediate terminal 2′,3′-*O*-cyclic phosphate is formed which in a second step is hydrolysed to produce a 3′-phosphate. Two histidine residues of RNase A (His12 and His119), located in the active site of the enzyme molecule, are involved in this process. 2′-CMP, although having a pyrimidine base, is *not* cleaved by RNase A by virtue of its 2′ (*not* 3′) linkage to the phosphate. Instead it inhibits the enzyme by simulating productive binding in the active site as confirmed in the present analysis.

* Correspondence author.

rical parameters describing the protein–inhibitor interactions, associated changes in the protein structure and reliable analysis of the solvent structure, particularly in the active-site region.

Experimental

Large native crystals, 0.5–1.0 mm in linear dimensions, using RNase A (Sigma) were grown as described by Carlisle, Palmer, Mazumdar, Gorinsky & Yeates (1974) from 30–40% ethanol at pH 5.2–5.7 and stored in 60% ethanol. The native crystals are monoclinic with unit-cell dimensions $a = 30.45\,(6)$, $b = 38.37\,(7)$, $c = 53.22\,(8)$ Å, $\beta = 106.0\,(5)°$, $P2_1$, $Z = 2$ ($M_r = 13\,685$). Suitable crystals were selected for diffractometry and soaked in a 20 mmol solution of cytidine-2′-phosphate (2′-CMP) for 12 h. The inhibitor solution was then removed and the capillary tube was sealed in the usual manner after positioning the monoclinic b axis of the crystal parallel to its length. [Intensity changes in the diffraction pattern had been previously established by Howlin *et al.* (1987).]

Using only one crystal of the complex, X-ray intensity data were collected by FAST diffractometry (Arndt, 1985) to approximately 1.6 Å resolution using the *MADNES* software (Messerschmidt & Pflugrath, 1987). An Elliot GX21 rotating-anode X-ray source running at 40 kV and 70 mA was used, data frames being collected in 40 s exposures at 0.1° steps over a 180° range. The crystal orientation was refined prior to and during data collection, allowing reflections to be integrated and Lp-corrected online. Data-collection details are given in Table 1(*a*). Merging of equivalents was performed with the Fox & Holmes (1966) algorithm by dividing the data into 5° batches on the scan angle (Ω), analogous to using separate films in the photographic method. The resulting measured structure-factor amplitudes $|F_{PI}|$, were combined with $|F_c|$ values derived from native ribonuclease-A coordinates (Borkakoti *et al.*, 1982).

Luzzati-weighted coefficients $(2m|F_{PI}| - D|F_c|)$ (Read, 1986) were prepared by the program *SIMWT* (Tickle, 1988), which also performs the derivative-to-native scaling. Prior to calculating difference electron-density maps, the protein side chains Glu11, His12, Lys41, Val43, Asn44, Thr45, Lys66, Phe120 and Ser123, in the vicinity of the active site and known to be highly labile, had been removed from the native-atom coordinate data set. Difference Fourier syntheses were calculated by the program *FFT* (Ten-Eyck, 1973) and displayed using *FRODO* (Jones, 1978) on an Evans and Sutherland PS390 raster graphics terminal. The initial maps allowed the inhibitor structure to be built in prior to least-squares refinement, which was performed with the program *RESTRAIN* (Haneef, Moss, Stanford & Borkakoti, 1985) using VAX and Convex computers. The complex structure was subjected to several rounds of re-building and restrained refinement. Refinement results are given in Table 1(*b*). The geometrical restraints libraries used by *FRODO* and *RESTRAIN* were extended to accommodate the geometrical features of the inhibitor molecule.

Table 1. *X-ray data and refinement statistics for RNase A–2′-CMP*

(*a*) X-ray data

	Native RNase A	RNase A–2′-CMP
Space group	$P2_1$*	$P2_1$
Cell constants		
a (Å)	30.45 (6)	30.51 (2)
b (Å)	38.37 (7)	38.24 (2)
c (Å)	53.22 (8)	53.30 (3)
β (°)	106.0 (5)	106.10 (2)
V (Å^3)	59771.7 (3)	59746.3 (1)
Wavelength λ(Cu $K\alpha$) (Å)	1.54	1.54
Crystal size (mm)	0.6 × 0.8 × 0.4	0.6 × 0.8 × 0.4
Total number of measured reflections	39576	
Number of unique reflections†	11945 (5650)‡	
Merging R factor§ (intensities)		

R_{merge}	Resolution (Å)
0.057	All data
0.040	6.71
0.038	4.74
0.040	3.87
0.044	3.35
0.052	3.00
0.064	2.74
0.065	2.54
0.104	2.37
0.078	2.24
0.086	2.12
0.089	2.02
0.114	1.94
0.129	1.86
0.154	1.79
0.164	1.73
0.184	1.68
0.203	1.63
0.227	1.54

Completeness of data to 1.6 Å (%)	76
Completeness of data 2.3–1.6 Å (%)	82
Completeness of data 1.8–1.6 Å (%)	74

(*b*) Refinement statistics

R.m.s. deviation from target bond lengths (Å)	0.022
R.m.s. deviation from target angle distances (Å)	0.051
R.m.s. distance from least-squares main-chain planes (Å)	0.024
R.m.s. deviation from least-squares side-chain planes (Å)	0.013
Mean coordinate error¶ (Å)	0.15
Resolution range (Å)	20.0–1.6
R factor (all data)	0.170
Number of cycles	120
Mean U_{iso}'s** for	
Enzyme (Å)	0.240 (955)
Inhibitor (Å)	0.233 (21)
Waters (Å)	0.427 (101)

* *International Tables for X-ray Crystallography* (1974, Vol IV).

† All unique data used throughout the analysis with no σ cut-off.

‡ 2.3 Å data set.

§ $R_{merge} = \sum_h \sum_i |I_{hi} - \langle I_h \rangle| / \sum_h N_h \langle I_h \rangle$, where h = reflection number, i = observation number, and N_h = number of observations of reflection h.

¶ Estimated from a Luzzati plot (Luzzati, 1952).

** Number of atoms is shown in parentheses.

Results and discussion

Conformational parameters of the bound inhibitor molecule 2′-CMP

The geometrical restraints imposed on the 2′-CMP molecule were designed to control the refinement of

bond lengths and bond angles, and to ensure planarity of the pyrimidine moiety. Since no other geometrical restrictions were used, conformational features, including the ribose puckering and the relative orientation of the base and sugar, *i.e.* the glycosidic torsion angle χ (or τ) = O(1′)—C(1′)—N(1)—C(2), were allowed to refine. According to Saenger (1984), from an extensive survey of crystal structures of ribonucleosides and their derivatives, the two most commonly observed modes of sugar puckering in such compounds are C(3′)-*endo* and C(2′)-*endo*, whilst the most heavily populated region of χ values is in the range 180–225° [for C(3′)-*endo* structures] and 215–260° [for C(2′)-*endo* structures]. In the present 1.6 Å refinement of the RNase–2′-CMP complex, the sugar puckering is C(3′)-*endo* (Table 2), and χ = 226 (4)°, *i.e.* very close to the preferred region for C(3′)-*endo* puckering.

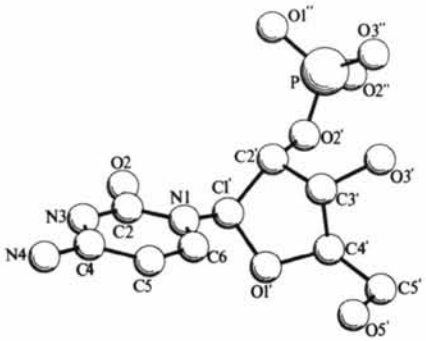

Fig. 2. Refined conformation of 2′-CMP inhibitor molecule, showing atomic numbering scheme.

Table 2. *Torsion angles* (°) *for the 2′-CMP inhibitor molecule*

N(1)—C(1′)—C(2′)—O(2′)	−159		C(4′)—O(1′)—C(1′)—C(2′)	1	
C(1′)—C(2′)—C(3′)—O(3′)	157		C(4′)—O(1′)—C(1′)—N(1′)	−121	
O(2′)—C(2′)—C(3′)—O(3′)	31		O(1′)—C(1′)—C(2′)—O(2′)	87	
C(1′)—C(2′)—C(3′)—C(4′)	48		O(1′)—C(1′)—C(2′)—C(3′)	−32	
O(2′)—C(2′)—C(3′)—C(4′)	−78	χ or τ_1	O(1′)—C(1′)—N(1)—C(2)	−134	(−115)*
C(2′)—C(3′)—C(4′)—C(5′)	173		P—O(2′)—C(2′)—C(1′)	147	(152)
C(2′)—C(3′)—C(4′)—O(1′)	−48		O(5′)—C(5′)—C(4′)—O(1′)	−49	(−86)
C(3′)—C(4′)—C(5′)—O(5′)	77		O(5′)—C(5′)—C(4′)—C(3′)	77	(137)
C(3′)—C(4′)—O(1′)—C(1′)	31		P—O(2′)—C(2′)—C(3′)	−100	(−92)
C(5′)—C(4′)—O(1′)—C(1′)	161		O(1)—P—O(2′)—C(2′)	−48	

* Values quoted from Howlin *et al.* (1987) in parentheses.

In the 2.3 Å resolution study of this inhibitor complex, the 2′-CMP molecule was reported to have similar conformational features, *i.e.* C(3′)-*endo* ribose puckering and χ = 245 (8)°. The difference in angles χ (19°) is around 3σ and may be considered insignificant. (Other examples of corresponding torsion angles between the two refined 2′-CMP molecules available to us are in Table 2.)

Protein–nucleotide interactions

Hydrogen bonds made between the inhibitor molecule and atoms in the protein structure, including

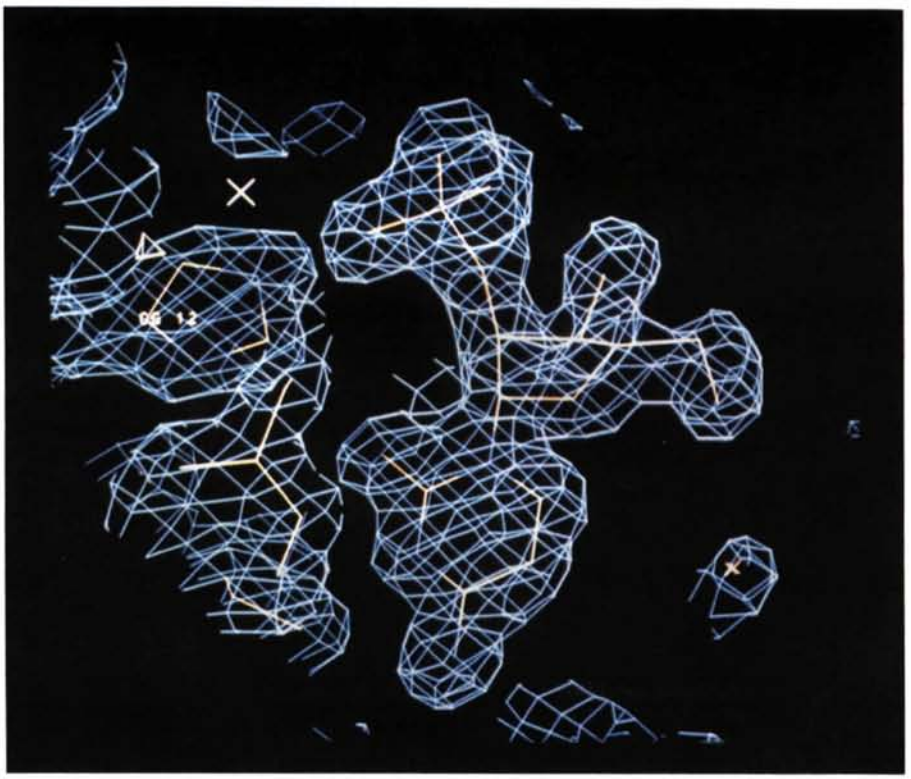

Fig. 3. Electron density of the base, ribose and phosphate and neighbouring protein groups.

solvent atoms, are shown in Fig. 5 and Table 3. Fig. 2 shows the conformation of the refined 2′-CMP inhibitor molecule. It was located, productively bound in the B1 pyrimidine site of the enzyme (Richards *et al.*, 1971) adjacent to Thr45, confirming the findings of Howlin *et al.* (1987). Fig. 3 shows the electron-density distribution in the active-site region. The cytidine base is held by interactions between its O(2) atom and the protein N(45) atom, between both N(3) and N(4) and protein Oγ (Table 3 and Fig. 4), all of which were observed in the 2.3 Å structure and to some extent in other RNase–inhibitor complex structures mentioned above.

Table 3. *Hydrogen-bonding distances* (<3.5 Å) *between inhibitor and protein atoms*

Inhibitor atom	Protein atom	Distance (Å)
O(1) phosphate	N 120	2.91*
O(1) phosphate	Nε2 12	2.63†
O(1) phosphate	O*W* 170	3.12*
O(2) phosphate	Nε2 11	2.88‡
O(3) phosphate	Nδ1 119	2.53‡
O(2′) ribose	O 43	3.16‡
O(2′) ribose	O*W* 174	3.04*
O(3′) ribose	O*W* 224	2.98*
O(5) ribose	O*W* 249	3.38*
O(2) base	N 45	3.02†
N(3) base	Oγ1 45	2.74†
N(4) base	Oγ1 45	3.45†

* Not reported in 2.3 Å structure.
† Corresponds to contact reported in 2.3 Å structure.
‡ Similar to contact reported in 2.3 Å structure.

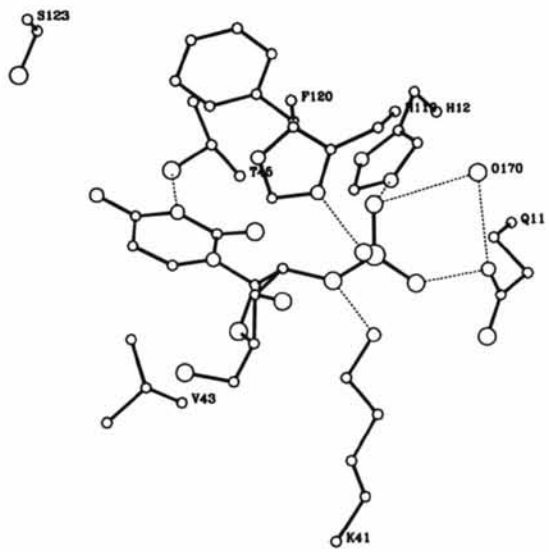

Fig. 4. RNase A–2′-CMP complex at 1.6 Å resolution, showing the refined positions of inhibitor, surrounding active site residues and hydrogen-bonding interactions.

As in the native structure, the electron density for the Glu11 side chain is well defined. Glu11 interacts with Lys7, Lys41 and the phosphate group of the inhibitor molecule. Contact between Glu11 and the phosphate group [also observed in O(3)-2′-CMP–RNase-A complex (Palmer *et al.*, 1984), and in the 2.3 Å 2′-CMP structure] is maintained within 3.5 Å, but contact is now indicated between atom O(3) of the phosphate and Nε2 of Glu11 instead of between O(3) of the phosphate and Oε1 of Glu11. There is no contact between Lys66 and the O(5′) of the ribose moiety or between the terminal nitrogen of Lys41 and O(3) of the phosphate, in keeping with the findings of the 2.3 Å structure analysis.

The active-site residues His12 and His119 are each in close proximity to one of the O atoms of the phosphate group (Fig. 4). Hydrogen-bond distances for the O(1) phosphate Nε2 of His12 and for the O(3) phosphate–Nδ of His119 are longer by 0.22 and 0.10 Å than the same bonds in the 2.3 Å structure, respectively. In view of the lower resolution of the

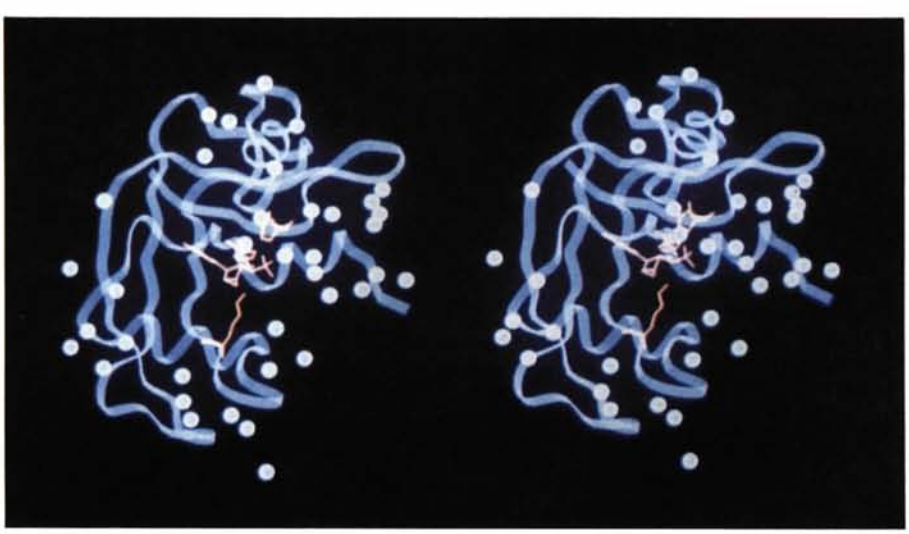

Fig. 5. Conserved solvent sites in five high-resolution RNase structures. The solvent cluster connecting the N-terminal α-helix with 110–121 loop is visible on the right-hand side of the molecule. The active site residues and the inhibitor are shown in red.

earlier analysis these differences are not significant. His119 occupies unambiguously the major *A* site (Borkakoti *et al.*, 1982) as also indicated by the 2.3 Å study. We have also confirmed the previous finding that there is no interaction between the inhibitor and the main-chain N atom of Phe120 which occurred in the cytidylyl-(2′,5′)-adenosine–RNase-A (CpA) structure of Wodak *et al.* (1977). However, several interactions between the cytidine base and the Phe120 side chain do occur, but there is no indication of base stacking between 2′-CMP and Phe120.

The importance of Lys41 in the mechanism of RNase A has been demonstrated (Jentoft, Gerkin, Jentoft & Dearborn, 1981) and several mechanisms suggesting possible functions of this residue have been reported (Usher, Erenrich & Eckstein, 1972; Griffin, Schachter & Cohen, 1973; Walter & Wold, 1976; Ruterjans & Witzel, 1969; Deakyne & Allen, 1979). Crystallographic studies have indicated (Richards & Wyckoff, 1973; Borkakoti *et al.*, 1982) that this residue is very labile and its precise location at the active site uncertain. In the 2.3 Å 2′-CMP structure the instability of this side chain is manifested in large temperature factors (the average mean-square displacement amplitude for the side-chain atoms U_{iso} is 0.62 Å^2), and in the diffuse appearance of the electron density for this side chain. However, in the present structure the density for Lys41 is well defined and the corresponding U_{iso} (average) is 0.24 Å^2 (Fig. 6). Nζ of Lys41 is at 4.66, 3.58 and 5.35 Å, respectively, from the phosphate O atoms O(1), O(2) and O(3).

The stabilization of the His119 side chain in the major *A* site in this structure confirms the same observation in the 2.3 Å analysis and is further evidence for the conformational flexibility of this side-chain group (Borkakoti *et al.*, 1982). In the O(3)-2′-CMP–RNase-A structure (Palmer *et al.*, 1984) the complex occupies solely the alternative *B* site. These observations support the argument that the lability of the His119 side chain may be necessary for the different roles it plays in the transphosphorylation and hydrolysis steps in the catalytic process of ribonuclease A. Torsion angles for His119, His12, Lys41 and Lys66 are given in Table 4. The Thr45 residue is, as in the 2.3 Å structure, very well resolved and can be quite unambiguously positioned. Binding of the inhibitor to RNase A appears not to produce a major movement of the side chain of Thr45.

Glu9 was found to exist in two conformations – a feature not apparent in the low-resolution structure.

Table 4. *Torsion angles* (°) *for the active-site histidine and lysine residues in the RNase A–2′-CMP complex*

For histidine χ_1 = N—Cα—Cβ—Cγ, χ_2 = Cα—Cβ—Cγ—Nδ and χ_2' = Cα—Cβ—Cγ—Cδ. For lysine χ_1 = N—Cα—Cβ—Cγ, χ_2 = Cα—Cβ—Cγ—Cδ, χ_3 = Cβ—Cγ—Cδ—Cε and χ_4 = Cγ—Cδ—Cε—Nζ.

(*a*) Histidine residues

	χ_1	χ_2	χ_2'
His12	−57	72	111
His119	157	68	−109

(*b*) Lysine residues

	χ_1	χ_2	χ_3	χ_4
Lys41	−168	178	156	175
Lys66	101	−179	−161	147

Solvent structure

(i) A total of 101 solvent molecules (O) were located and refined, criteria for acceptance being through hydrogen-bond formation and U_{iso} value less than 0.80 Å^2. This compares with 85 solvent atoms located in the 2.3 Å analysis (Howlin *et al.*, 1987).

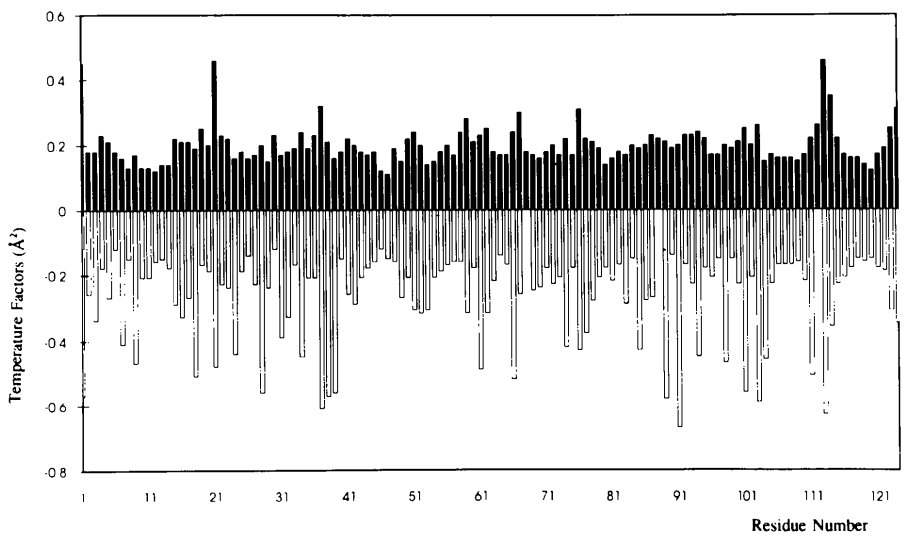

Fig. 6. Histogram of main-chain (upper) and side-chain (lower) temperature factors.

(ii) Conserved solvent sites. The solvent coordinates of different RNase-A structures (Table 5) were compared with positions located in the RNase-A 2′-CMP complex described here. The structures were superimposed by least-squares refinement of the positions of the backbone atoms. Solvent sites were considered as conserved when water molecules were present within a sphere of 0.5 Å radius in three or more structures.

Four structures of RNase A were compared with the 2′-CMP complex described here (Table 5). A number of water molecules were found in conserved positions, forming similar hydrogen bonds in the different structures. 37 solvent sites were conserved in all five structures, 18 solvent sites in four out of five structures, and 30 sites were conserved in three of the structures (Fig. 5). Six of those conserved waters are involved in intermolecular contacts between symmetry-related molecules, and may be determined by the crystal environment. The 37 highly conserved sites are found in clusters on the surface of the protein, and many forming hydrogen bonds with backbone amide and carbonyl groups that are solvent exposed. A major group of conserved waters surrounds the N-terminal α-helix (residues 1–22), filling all the solvent-exposed clefts that surround it. These waters probably play an important role in stabilizing this part of the protein, as the α-helix has relatively few direct contacts with other secondary-structure elements. An important cluster of sites connects the N-terminal α-helix with the loop 110–121 (Fig. 5). These two secondary-structure elements contain the histidine groups 12 and 119 that are responsible for the cleavage of RNA.

(iii) Active-site hydration. The inhibitor bound in the active site displaces six of the water molecules found in the active site of the phosphate-free 1.26 Å structure of RNase A (Wlodawer, Svenson, Sjölin & Gilliland, 1988). A CMP phosphate O atom occupies the same position as water 203 from the phosphate-free RNase A, and forms a similar hydrogen bond to His12. N(3) of the pyrimidine ring takes the position of water 240, forming a hydrogen bond with Oγ1 of Thr45, and the pyrimidine O(2) takes the place of a water that interacts with N(45) of Thr45. Two conserved solvent sites are in direct contact with the inhibitor, forming hydrogen bonds with the ribose O(1′) and the phosphate O(1).

Concluding remarks

Although very similar, the two structures for RNase A–2′-CMP (2.3 Å, Howlin *et al.*, 1987) and the present 1.6 Å resolution analysis show some important differences. In particular in the 1.6 Å structure the catalytically important Lys41 side chain is now clearly defined, as is also the ribose moiety of the 2′-CMP inhibitor molecule. As a consequence of the latter observation, significant improvement in the conformational parameters of the inhibitor (Table 2) has now been achieved. Many solvent molecules in the 1.6 Å analysis are clearly located, resulting in a further 16 being included successfully in the refinement. Finally, the 1.6 Å analysis has confirmed the binding of 2′-CMP as the only productively bound RNase inhibitor reported to date.*

Table 5. *High-resolution monoclinic $P2_1$ RNase-A crystal structures used to establish conserved solvent sites*

	RNase PF	RNase A	RNase XF	RNase V	RNase–2′-CMP
Coordinate set*	7RSA	3RN3	5RSA	6RSA	(This structure)
Precipitating agent	2-Methyl-2-propanol	40% Ethanol	2-Methyl-2-propanol	2-Methyl-2-propanol	40% Ethanol
pH	5.3	5.2–5.7	5.3	5.3	5.3
Resolution (Å)	1.26	1.45	2.0	2.0	1.6
No. of solvent molecules located	188	127	196	221	101
R value	0.150	0.223	0.159 (X-ray) 0.188 (Neutron)	0.188 (X-ray) 0.199 (Neutron)	0.170

Notes: RNase PF: phosphate-free RNase A (Wlodawer, Svenson, Sjölin & Gilliland, 1988). RNase A: X-ray structure (Borkakoti, Moss & Palmer, 1982). RNase XF: joint X-ray/neutron structure (Wlodawer & Sjölin, 1983). RNase V: uranyl vanadate complex (Wlodawer, Miller & Sjölin, 1983).

* Brookhaven PDB reference (Bernstein *et al.*, 1977).

* Atomic coordinates and structure factors have been deposited with the Protein Data Bank, Brookhaven National Laboratory. Free copies may be obtained through The Technical Editor, International Union of Crystallography, 5 Abbey Square, Chester CH1 2HU, England (Supplementary Publication No. SUP 37094). A list of deposited data is given at the end of this issue.

References

AGUILAR, C. F., THOMAS, P. J., MOSS, D. S., MILLS, A. & PALMER, R. A. (1992). *J. Mol. Biol.* **224**, 265–267.

ARNDT, U. W. (1985). *Methods Enzymol.* **114**, 472–485.

BERNSTEIN, F. C., KOETZLE, T. F., WILLIAMS, G. J. B., MEYER, E. F. JR, BRICE, M. D., ROGERS, J. R., KENNARD, O., SHIMANOUCHI, T. L. & TASUMI, M. (1977). *J. Mol. Biol.* **112**, 535–542.

BLACKBURN, P. & MOORE, S. (1982). *The Enzymes*, 3rd ed., Vol. XV, Part B, edited by P. D. BOYER. New York: Academic Press.

BORKAKOTI, N., MOSS, D. S. & PALMER, R. A. (1982). *Acta Cryst.* B**38**, 2210–2217.

BORKAKOTI, N., PALMER, R. A., HANEEF, N. & MOSS, D. S. (1983). *J. Mol. Biol.* **169**, 743–755.

CARLISLE, C. H., PALMER, R. A., MAZUMDAR, S. I., GORINSKY, B. A. & YEATES, D. G. R. (1974). *J. Mol. Biol.* **85**, 1–18.

DEAKYNE, C. A. & ALLEN, L. G. (1979). *J. Am. Chem. Soc.* **100**, 7394–7402.

FOX, G. C. & HOLMES, K. C. (1966). *Acta Cryst.* **20**, 886–891.

GRIFFIN, J. H., SCHACHTER, A. N. & COHEN, J. S. (1973). *Ann. N. Y. Acad. Sci.* **222**, 693–708.

HANEEF, I., MOSS, D. S., STANFORD, M. J. & BORKAKOTI, N. (1985). *Acta Cryst.* A**41**, 426–433.

HOWLIN, B., HARRIS, G. W., MOSS, D. S. & PALMER, R. A. (1987). *J. Mol. Biol.* **196**, 159–164.

JENTOFT, J. E., GERKIN, T. A., JENTOFT, N. & DEARBORN, D. G. (1981). *J. Biol. Chem.* **256**, 231–236.

JONES, T. A. (1978). *J. Appl. Cryst.* **11**, 268–272.
LUZZATI, V. (1952). *Acta Cryst.* **5**, 802–810.
MESSERSCHMIDT, A. & PFLUGRATH, J. W. (1987). *J. Appl. Cryst.* **20**, 306–315.
PALMER, R. A., MOSS, D. S., HANEEF, I. & BORKAKOTI, N. (1984). *Biochim. Biophys. Acta*, **785**, 81–88.
PAVLOVSKY, A. G., BORISOVA, S. N., BORISOV, V. V., ANTONOV, I. V. & KARPEISKY, M. Y. (1978). *FEBS Lett.* **92**, 258–262.
READ, R. J. (1986). *Acta Cryst.* **A42**, 140–149.
RICHARDS, F. M. & WYCKOFF, H. W. (1973). In *Atlas of Molecular Structures in Biology*, Vol. 1, *Ribonuclease S*, edited by D. C. PHILLIPS & F. M. RICHARDS. Oxford: Clarendon Press.
RICHARDS, F. M., WYCKOFF, H. W., ALLEWELL, N. M., LEE, B. & MITSUI, Y. (1971). *Cold Spring Harbour Symp. Quant. Biol.* **36**, 35–43.
RUTERJANS, H. & WITZEL, H. (1969). *Eur. J Biochem.* **9**, 118–127.
SAENGER, W. (1984). *Principles of Nucleic Acid Structure*. Heidelberg: Springer-Verlag.
TEN-EYCK, L. F. (1973). *Acta Cryst.* **A29**, 183–191.
TICKLE, I. J. (1988). *Improving Protein Phases*, edited by S. BAILEY, E. DODSON & S. PHILLIPS, pp. 130–137. Warrington, England: SERC Daresbury Laboratory.
USHER, D. A., ERENRICH, A. & ECKSTEIN, F. (1972). *Proc. Natl Acad. Sci. USA*, **69**, 115–118.
WALTER, B. & WOLD, F. (1976). *Biochemistry*, **15**, 304–310.
WLODAWER, A., MILLER, M. & SJÖLIN, L. (1983). *Proc. Natl Acad. Sci. USA*, **80**, 3628–3631.
WLODAWER, A. & SJÖLIN, L. (1983). *Biochemistry*, **22**, 2720–2728.
WLODAWER, A., SVENSON, L. A., SJÖLIN, L. & GILLILAND, G. L. (1988). *Biochemistry*, **27**, 2705–2717.
WODAK, S. Y., LIU, M. Y. & WYCKOFF, H. W. (1977). *J. Mol. Biol.* **116**, 855–875.